



## RESEARCH LETTER

10.1029/2021GL097107

## Small-Scale Irregularities Within Polarization Jet/SAID During Geomagnetic Activity

A. A. Sinevich<sup>1,2</sup> , A. A. Chernyshov<sup>1,2</sup> , D. V. Chugunin<sup>1</sup>, A. V. Oinats<sup>3</sup> , L. B. N. Clausen<sup>4</sup> , W. J. Miloch<sup>4</sup> , N. Nishitani<sup>5</sup> , and M. M. Mogilevsky<sup>1</sup>

<sup>1</sup>Space Research Institute of the Russian Academy of Science, Moscow, Russia, <sup>2</sup>National Research University Higher School of Economics, Moscow, Russia, <sup>3</sup>Institute of Solar Terrestrial Physics, SB RAS, Irkutsk, Russia, <sup>4</sup>Department of Physics, University of Oslo, Oslo, Norway, <sup>5</sup>Institute for Space-Earth Environmental Research, Nagoya University, Nagoya, Japan

### Key Points:

- Fluctuations of plasma parameters inside the polarization jet (PJ) increase at all scales during higher geomagnetic activity
- Small-scale irregularities inside the PJ are measured in situ down to hundreds of meters
- The role of large-scale effects in the PJ increases in comparison with small-scale ones with geomagnetic activity

### Correspondence to:

A. A. Sinevich,  
sinevich.aa@gmail.com

### Citation:

Sinevich, A. A., Chernyshov, A. A., Chugunin, D. V., Oinats, A. V., Clausen, L. B. N., Miloch, W. J., et al. (2022). Small-scale irregularities within polarization jet/SAID during geomagnetic activity. *Geophysical Research Letters*, 49, e2021GL097107. <https://doi.org/10.1029/2021GL097107>

Received 18 NOV 2021

Accepted 7 APR 2022

**Abstract** We study the spatial structure of a polarization jet/Sub-Auroral Ion Drift (PJ/SAID) based on data from the NorSat-1 and Swarm satellites during a geomagnetic storm. Observations of plasma parameters inside the PJ/SAID are obtained with NorSat-1 using a system of Langmuir probes with a nominal sampling rate of up to 1 kHz, which allowed measurements with such a high temporal resolution for the first time. A comparative analysis of plasma parameters and electron density spectra inside PJ according to the data from both satellites is presented. Our results show that fluctuations of plasma parameters inside the PJ increase at all scales with increasing geomagnetic activity. Small-scale irregularities in the PJ are measured in situ down to hundreds of meters. The role of large-scale effects in the PJ increases in comparison with the small-scale ones during high geomagnetic activity. The PJ consists of structures  $\sim 0.2^\circ$  latitude in size within which small-scale irregularities are present.

**Plain Language Summary** Polarization jet (PJ), also known as Sub-Auroral Ion Drift (SAID), events are fast westward plasma drifts with a narrow latitudinal extent, occurring at subauroral latitudes in the Earth's ionosphere. The decrease in the density of the ionospheric plasma inside PJ/SAID significantly affects the conditions for the propagation of shortwave radio waves, which indicates the practical importance of studying this phenomenon. Despite the importance of using a variety of ground-based observation facilities for studying and analyzing PJ/SAID properties, as well as developing analytical models and numerical modeling, in situ observations are the most valuable. Such in situ observations can be obtained only with satellites flying through a developing PJ/SAID. Large-scale features of PJ/SAID are currently well understood, but small-scale processes within PJ/SAID are practically not studied, and many open questions remain. In this work, we study the small-scale structures in PJ/SAID during a geomagnetic storm of 20 April 2018, using multi-instrumental approach involving low-Earth orbit.

## 1. Introduction

In the subauroral ionosphere, there are often observed narrow streams of fast subauroral ion drift to the west near the projection of the plasmopause at the height of the F-layer of the ionosphere. They are most noticeable during storms/substorms on the background of the large-scale plasma convection (Anderson et al., 1991; Foster et al., 2002). For the first time, such streams were recorded with the Soviet satellite Kosmos-184, and they were called “polarization jet” (PJ; Gal'perin et al., 1973, 1974). In the scientific literature, this phenomenon was also called “SubAuroral Ion Drifts” (SAIDs) after the paper of Spiro et al. (1979) where narrow streams of ion drifts were studied using data from the American satellite Atmosphere Explorer C (AE-C). The bandwidth of PJ/SAID at ionospheric heights is  $1^\circ$ – $2^\circ$  in latitude, and the drift velocity is  $\sim 1$  km/s and more in the westerly direction and is recorded in the evening and night MLT sectors. At the same time, broad flows are encountered in the evening sector ( $< 20$  MLT; Figueiredo et al., 2004; Karlsson et al., 1998; Yeh et al., 1991). Foster and Burke (2002) combined these two types of observations of subauroral electric fields: narrow jets of ion drift (PJ) and wide regions of ionospheric convection to the west with high velocities, called SubAuroral Polarization Stream (SAPS). These phenomena (SAPS and PJ) were studied with the satellite data, measurements by a chain of ground-based ionospheric stations, SuperDARN HF radars, and with the coherent scattering of radio signals (e.g., de Keyser, 2000; Gallardo-Lacourt et al., 2017; Galperin, 2002; Khalipov et al., 2016; Koustov et al., 2006; Makarevich et al., 2011; Mishin, 2013; Mishin et al., 2017; Nishitani et al., 2019; and Stepanov et al., 2019, 2017 among others).

© 2022. The Authors.

This is an open access article under the terms of the Creative Commons Attribution-NonCommercial-NoDerivs License, which permits use and distribution in any medium, provided the original work is properly cited, the use is non-commercial and no modifications or adaptations are made.

Despite the importance of using a variety of ground-based observations for studying and analyzing the properties of PJ/SAPS, as well as the development of analytical and numerical models, the most valuable are in situ observations, which can be obtained only with a satellite flying through the subauroral region during PJ/SAPS development. For example, besides above-mentioned Kosmos-184 and AE-C, such satellites as S3-2 (Smiddy et al., 1977), OGO-6 (Maynard, 1978), DE-1 and DE-2 (Anderson et al., 1993), CRESS (Burke et al., 1998, 2000; Rowland & Wygant, 1998), Swarm (Archer et al., 2019), IMAGE (Goldstein et al., 2003), and AMPTE/CCE (Khalipov et al., 2003) were used. A large number of studies of PJ/SAPS are based on data from the DMSP series of satellites (e.g., Anderson et al., 2001; Foster & Burke, 2002; Foster & Vo, 2002; and Mishin et al., 2003 among others). Using the data from these satellites, interesting cases were found when two peaks of PJ velocities were observed side by side on one satellite pass, that is, the so-called Double-peak SAID (DSAID; He et al., 2016). These results were later confirmed by Wei et al. (2019) with not only DMSP measurements but also Van Allen Probes (RBSP) and in Sinevich et al. (2021) using the NorSat-1 data.

Thus, comprehensive studies involving various space missions made it possible to identify the main large-scale features in the formation and development of PJ and SAPS, to determine the time and place where subauroral ion drifts appear with the maximum probability as well as their relationship with geomagnetic disturbances. However, many satellites were not equipped with instruments that would allow for a deeper study of characteristics of electromagnetic and plasma perturbations in the upper F-layer ionosphere at subauroral latitudes during PJs or the satellite scientific payload did not allow for measurements at high spatiotemporal resolution. Small-scale processes within PJ or SAPS have in effect not been well studied, and many open issues remain here. In this work, we use data from the NorSat-1 microsatellite, which measured parameters of ionospheric plasma in situ with Langmuir probes (LPs) with a maximum sampling rate of up to 1 kHz, while the spherical LP on the Swarm satellite has a resolution of 2 Hz. This makes it possible to study the small-scale structure in PJ in the subauroral region during increased geomagnetic activity, which is the main goal of this study of PJ/SAID, in which we use data from the NorSat-1 and Swarm satellites.

## 2. Satellite Data

The Norwegian microsatellite NorSat-1 (~16 kg, 23 × 39 × 44 cm) was launched on 14 July 2017, from the cosmodrome of Baikonur into a circular sun-synchronous orbit with an inclination of 98°, altitude of ~600 km, and orbital period of 95 min. The satellite has a multi-needle Langmuir Probe (m-NLP) developed at the University of Oslo. The m-NLP consists of four cylindrical probes (needles) at different voltage bias within the electron saturation region of the current-voltage characteristic (Hoang et al., 2018). To determine the electron density  $N_e$  in measurements by the system of LPs, at least two cylindrical probes operating at different fixed voltages are used (Jacobsen et al., 2010):

$$N_e = \frac{1}{KA} \sqrt{\frac{\Delta(I_c)^2}{\Delta V_b}} \quad (1)$$

where  $K$  is the constant equal to  $\frac{e^{3/2}}{\pi} \sqrt{\frac{2}{m_e}}$ ;  $\Delta(I_c)^2$  is the difference of squared collected currents;  $A$  is the surface area of the probe; and  $\Delta V_b$  is the probe voltage difference.

A key feature of m-NLP approach is that it does not need information about plasma potential and electron temperature to measure the electron density. The electron temperature in eV is calculated from the following formula:

$$T_e = \frac{R(V_s + V_{p2}) - (V_s + V_{p1})}{1 - R} \quad (2)$$

where  $V_s$  is the satellite potential;  $V_{p1}$  and  $V_{p2}$  are the fixed potentials of probes;  $R = I_{c1}^2 / I_{c2}^2$  where  $I_{c1}$  and  $I_{c2}$  are the currents measured by probes, which are at potentials  $V_{p1}$  and  $V_{p2}$ , respectively. Since we do not know the satellite potential, we cannot calculate accurate temperature values from this formula for the region of electron saturation of the current-voltage characteristic of the LPs. However, while the absolute electron temperature cannot be derived without knowing the satellite potential in accordance with the Langmuir probe theory, we can estimate the change of temperature with time and latitude (Chernyshov et al., 2020).

The European Space Agency's three Swarm satellites were launched on 22 November 2013 into nearly polar, circular orbits, eventually reaching altitudes of 460 km (Alpha and Charlie) and 510 km (Bravo). The Swarm mission is to make precise multipoint measurements of low-frequency magnetic and electric fields in the Earth's ionosphere. The values of electron density and temperature are measured by two spherical LPs installed on the satellites (Knudsen et al., 2017).

### 3. Measurement Results Analysis

This study details the geomagnetic storm of 20 April 2018 when there were successful passages of the NorSat-1 and Swarm-C satellites across the same PJ, which allows a comprehensive study of the plasma streams dynamics at subauroral latitudes. Figure 1a shows the evolution of the geomagnetic indices Dst (left vertical axis) and SME (right vertical axis) during the storm. The abscissa shows the time interval from 12 UT on 19 April 2018 to 12 UT on 21 April 2018. This interval was chosen so that both the main phase of the storm and its recovery phase could be seen in the Dst plot. Blue and red arrows in Figure 1a indicate times at which the PJ was detected in each of the considered passages of Swarm-C and NorSat-1, respectively. Therefore, we can see that the storm recovery phase on 20 April 2018, began at ~09 UT. The first PJ recorded by both spacecrafts at 10 UT occurred just during the storm recovery phase.

Figure 1b demonstrates the passages of the NorSat-1, Swarm-C, and DMSP F-17 satellites in MLAT-MLT coordinates. It can be seen from this figure that the NorSat-1 and Swarm-C passages are 2 hr MLT apart. Taking into account the fact that, on average, the PJ covers ~6 hr MLT (Karlsson et al., 1998) and the passages coincide in time (the difference is 6 min in the case of the first passage), we can assume that the PJ present at the moment of the NorSat-1 passage is also present at the time of the Swarm-C passage.

In this work, we use the DMSP F-17 satellite in situ ion drift velocity measurements and the SuperDARN Doppler velocity data in order to explicitly prove that a PJ occurred during this storm. DMSP F-17 flew at an altitude of ~849 km from the equator toward the northern polar region in ~18 MLT sectors at ~10:40 UT and its electron density and horizontal ion drift velocity measurements are presented in Figure 1c. It is clear that in the interval 58.2–60.3 MLAT (i.e., 10:39:42–10:40:25 UT) marked with a gray area, the electron density dip ~2.2° width in latitude coincides with an increase in drift velocity. It is worth noting that the ion drift velocity inside considered electron density dip exceeds 1,000 m/s, which is the typical drift velocity of PJ (Anderson et al., 1991) in the interval of ~1° of latitude width that is the characteristic for PJ (Karlsson et al., 1998). Moreover, the location of 18 MLT and 60 MLAT is also typical for PJ (Spiro et al., 1979). Thus, we conclude that DMSP F-17 crossed the PJ in the considered time interval. Furthermore, we assume that this is the same PJ that was found indirectly by NorSat-1 because the difference in MLT between satellites of ~7 hr can be explained by the fact that the PJ is usually elongated along the Soft Electron Boundary (SEB) and lies between 18 MLT and 02 MLT (Spiro et al., 1979). The difference in time of ~30 min can be explained by the fact that the typical duration of PJ is between 30 min and 3 hr (Anderson et al., 1991). Also, the difference in MLAT of 7° is due to the fact that according to Figure 1a after ~10:10 UT, the significant drop in geomagnetic activity occurred and according to Karlsson et al. (1998), the average MLAT of the PJ increases with a decrease in geomagnetic activity. Additionally, ionospheric plasma drift velocity measurements provided by the SuperDARN radars at heights of the F2 ionosphere region (~300 km) are presented in Figures 1d and 1e. The arrow in Figure 1d indicates the band of westward plasma drifts 1°–2° of latitude wide with Doppler velocities of 500–1,500 m/s observed by the #7–#10 HOK beams at 10:46 UT, which is almost at the same time as the PJ found using DMSP F-17 data. The arrows in Figure 1e illustrate the bands of strong westward plasma drifts 2°–4° of latitude wide exceeding 1,200 m/s observed by both the ADW and ADE radars at 07:47 UT which the moment of ~1 hr after one of the most significant rises in geomagnetic activity for the storm that occurred in ~06:40 UT. Note that since SuperDARN radars measure velocity projection onto beam direction, the actual plasma velocity could be significantly greater than those shown on Figures 1d and 1e, depending on the angle between beam direction and the actual plasma drift velocity vector (Nishitani et al., 2019). Thus, it is evidently shown that PJ exists during this geomagnetic storm.

Figures 2a and 2b shows a comparison of the electron density and temperature according to data from NorSat-1 and Swarm-C during the first considered joint passage. Both satellites were in the northern hemisphere and flew from the pole toward the equator in sectors of ~01 MLT and ~02 MLT for NorSat-1 and Swarm-C, respectively. In UT time, the passage of NorSat-1 in the region shown lags behind the passage of Swarm-C by ~6 min. Since

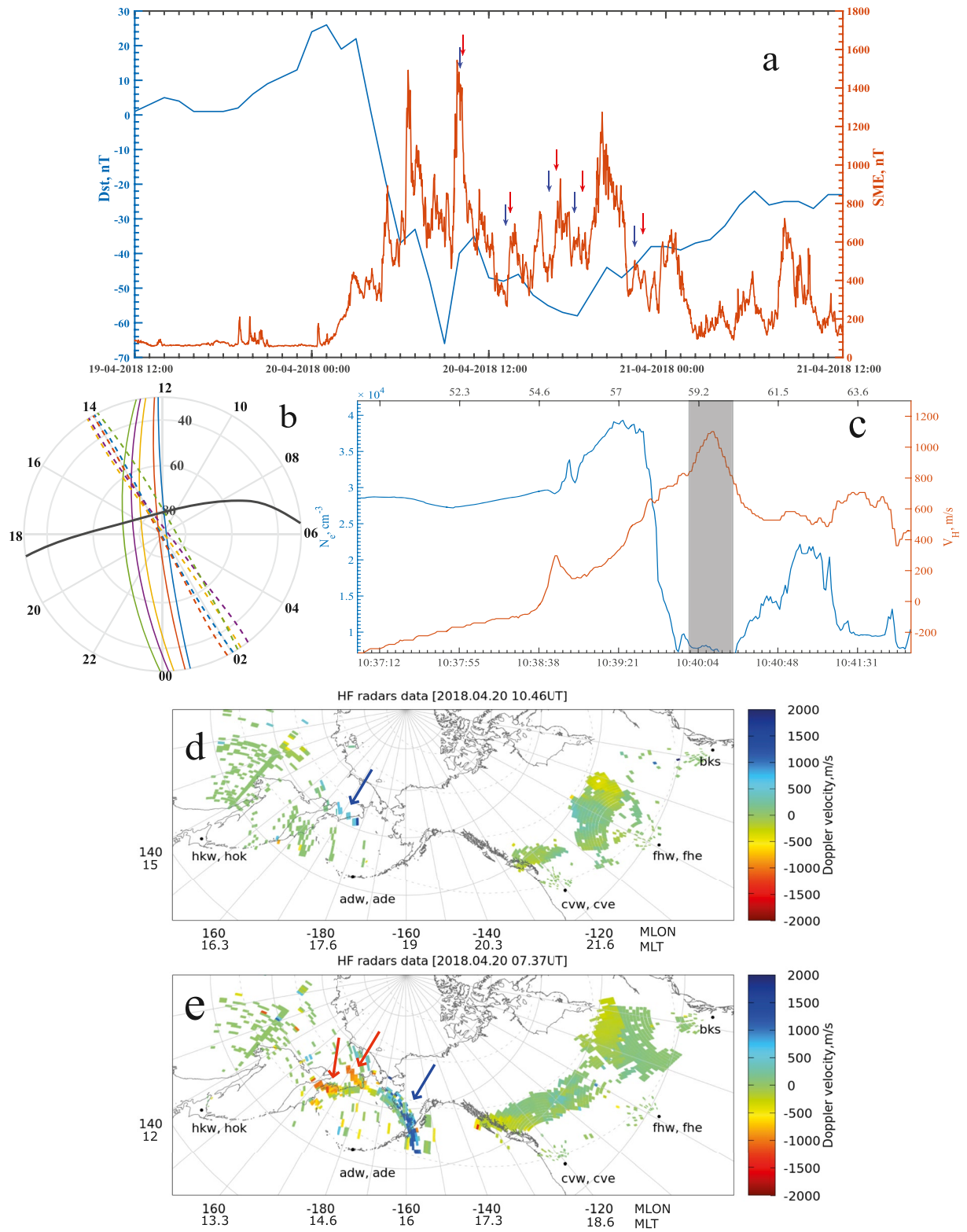
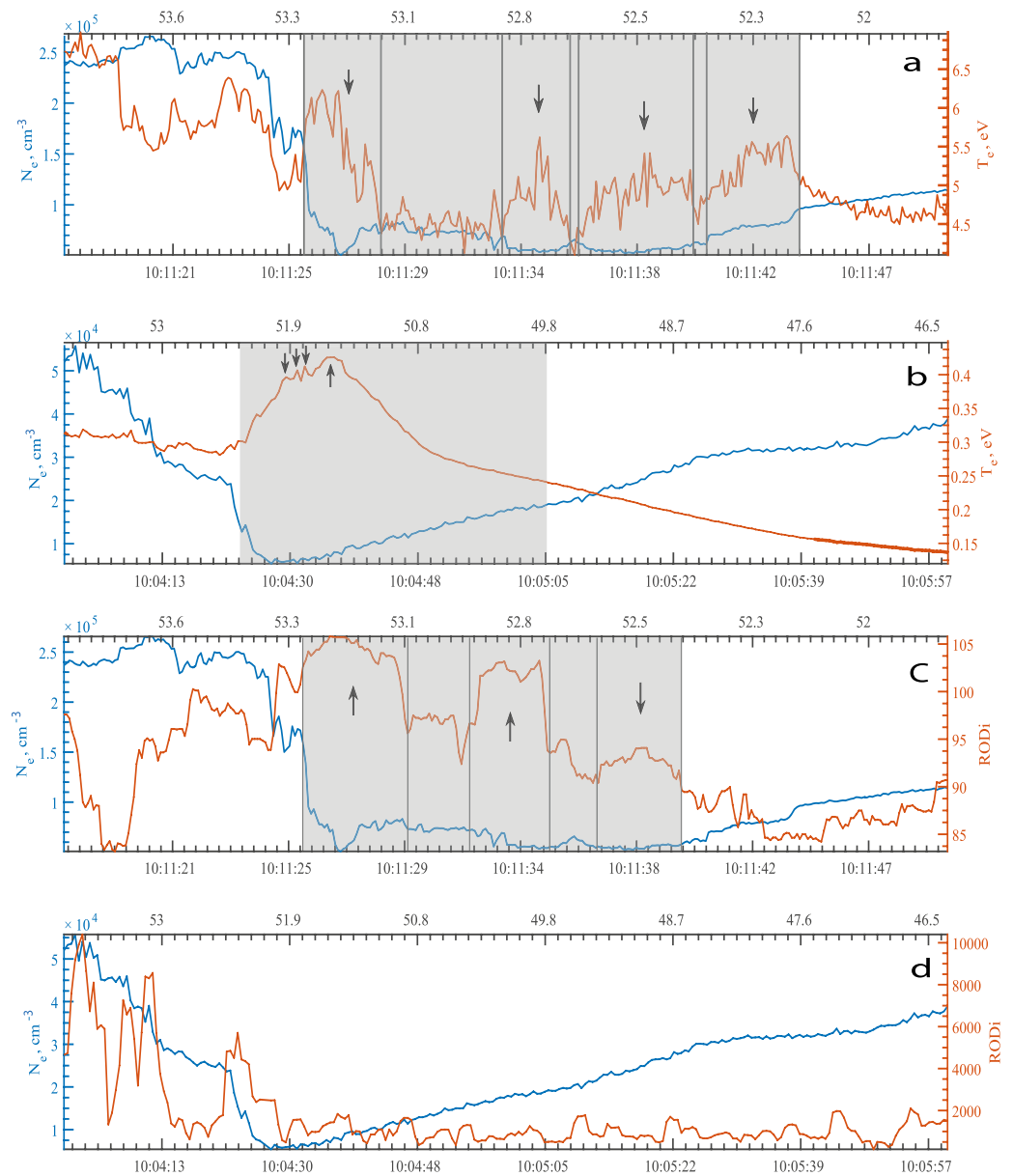


Figure 1.



**Figure 2.** Evolution of the temperature and electron density during the NorSat-1 passage at 10:11:18–10:11:51 UT on 20 April 2018 (a) and the Swarm-C passage (b) at 10:03:48–10:04:58 UT. The left vertical axis is the electron density and the right vertical axis is the electron temperature. The upper horizontal axis is the invariant latitude and the lower horizontal axis is the UT time. Evolution of the rate of change of density index (RODI) and electron density during the NorSat-1 passage (c) and the Swarm-C passage (d). RODI is calculated in a 0.1 s running window for NorSat-1 and in 2 s running window for Swarm-C. Gray areas highlight the position of the polarization jet (PJ). Arrows indicate small temperature (a, b) and RODI (c) peaks, which can be interpreted as strata of the PJ.

the measurements are performed with a nominal sampling rate of  $\sim 1$  kHz, the plots show the NorSat-1 measurements averaged over 100 points, that is, the moving average procedure has been applied to data.

**Figure 1.** (a) Dst and SME indices from 12 UT 19 April 2018 to 12 UT 21 April 2018. Arrows indicate the times at which a polarization jet was detected in each of the considered passages of NorSat-1 (red) and Swarm-C (blue). (b) Trajectories of the considered satellite passages in MLAT-MLT coordinates. Lines indicate the first to fifth passages of NorSat-1 (solid color), Swarm-C (dashed), and DMSP F-17 (solid black). (c) Evolution of horizontal ion drift velocity (red line) and electron density (blue line) during the DMSP F-17 passage at 10:37:00–10:42:00 UT. (d, e) Doppler velocity data from SuperDARN radars at 10:46 UT (d) and at 07:37 UT (e). Red areas indicated by red arrows show westward drift velocities measured by ADWR radar, blue areas indicated by blue arrows show westward drift velocities measured by HOK (d) and ADE (e) radars. Geographic latitudes indicated by solid contours, geomagnetic latitudes shown by dashed contours.

The top panel of Figure 2 shows that at  $\sim 53.3$  MLAT at 10:11:25 UT, the electron density decreases by a factor of  $\sim 2$ . Figure 2b also shows a decrease in the electron density by  $\sim 1.5$  times at  $\sim 52.4$  MLAT at 10:04:23 UT and then a gradual recovery to the previous values after  $\sim 51.9$  MLAT at 10:04:30 UT. Taking into account the above and the fact that both satellites at this moment moved from the polar cap region toward the southern hemisphere crossing the subauroral region of the ionosphere (50–70 MLAT), it can be confidently asserted that both satellites in the time interval shown in Figure 2 crossed SEB and Main Ionospheric Trough (MIT). This is in accordance with the current understanding that the PJ is located inside the MIT, often at its polar wall, on the SEB (Anderson et al., 1991). On the top panel of Figure 2 inside the MIT, it can be seen that in the interval 53.3–52.2 MLAT (i.e., 10:11:25–10:11:44 UT), adjacent to the polar wall of the MIT, the electron density dip coincides with an increase in the electron temperature. Figure 2b shows a similar effect: the interval 52.4–50.8 MLAT (i.e., 10:04:23–10:04:48 UT) is adjacent to the polar wall of the MIT and inside this interval the dip in the electron density and the increase in the electron temperature coincide. Thus, using these indirect evidences, we can confirm that NorSat-1 and Swarm-C crossed the PJ during the first considered joint passage.

Note that according to Figures 2a and 2b, the NorSat-1 densities are 5 times higher than the Swarm-C data. This is because there is some inaccuracy with the absolute density measurements with NorSat-1; however, the relative changes in electron density are measured accurately. In the upper panel of Figure 2, inside the highlighted by gray areas PJ, due to the high sampling rate of NorSat-1, small-scale fluctuations in the electron temperature are visible as well as four local density drops coinciding with the temperature rise which is of  $\sim 0.2$  MLAT in width (indicated by arrows), the most pronounced of which is located at the polar wall of the PJ. This result allows us to assume that the inner part of PJ consists of strata. However, verifying this hypothesis requires further studies of the small-scale structure of PJ.

Moreover, Figure 2b shows that inside the PJ at  $\sim 51.8$  MLAT (10:04:32 UT), there are three small temperature peaks with a width of  $\sim 0.1$  MLAT as well as a small temperature rise with a width of  $\sim 0.2$  MLAT at  $\sim 51.6$  MLAT (10:04:35 UT). These temperature peaks and rises inside the PJ measured by Swarm-C with a sampling rate of 2 Hz and indicated in the figure by arrows are similar in size and location to the plasma density drops inside the PJ measured by NorSat-1 with a sampling rate of 1 kHz. Therefore, it can be concluded that these two effects observed may be the same phenomenon, measured with different sampling frequency. The temperature and electron density obtained with the NorSat-1 data are in good agreement with the variations of these parameters as measured with Swarm-C, which reaffirm that the measurements with both satellites are correct.

It may also be inferred from Figures 2a and 2b that the position of the PJ during the passage of NorSat-1 ( $\sim 53.3$ – $52.2$  MLAT) differs from the position of the PJ during the passage of Swarm-C ( $\sim 52.4$ – $50.8$  MLAT) by  $\sim 1.2$  MLAT. Considering that the difference in MLT between NorSat-1 and Swarm satellites is 2 hr, the difference in MLAT of the PJs can be explained by the fact that in accordance with Karlsson et al. (1998) (their Plate 1), the mean MLAT of PJ decreases linearly with an increase in MLT toward the morning sector at a rate of  $\sim 0.55$  per hr. Moreover, Foster and Vo (2002) state that the mean latitude of SAPS (which is often located on same latitudes as PJ) is seen to decrease linearly at a rate of  $\sim 0.7$  per hr of MLT. It also explains why the westward PJ/SAID flow in Figure 1e extends from  $\sim 50$  MLAT according to HOK and ADE radars to  $\sim 60$  MLAT according to ADW.

To analyze in detail the small-scale irregularities, we employ the rate of change of density index (RODI). RODI is a parameter that indicates structuring of the plasma within a specified interval (Jin et al., 2019). RODI is the standard deviation of Rate of change of Density (ROD) in a running window:

$$RODI(t) = \sqrt{\frac{1}{N-1} \sum_{t_i=t-\Delta t/2}^{t_i=t+\Delta t/2} |ROD(t_i) - \overline{ROD}|^2} \quad (3)$$

where  $\overline{ROD}$  is the mean of  $ROD(t_i)$ :

$$\overline{ROD} = \frac{1}{N} \sqrt{\sum_{t_i=t-\Delta t/2}^{t_i=t+\Delta t/2} ROD(t_i)} \quad (4)$$

ROD is defined as a time derivative of the electron density:

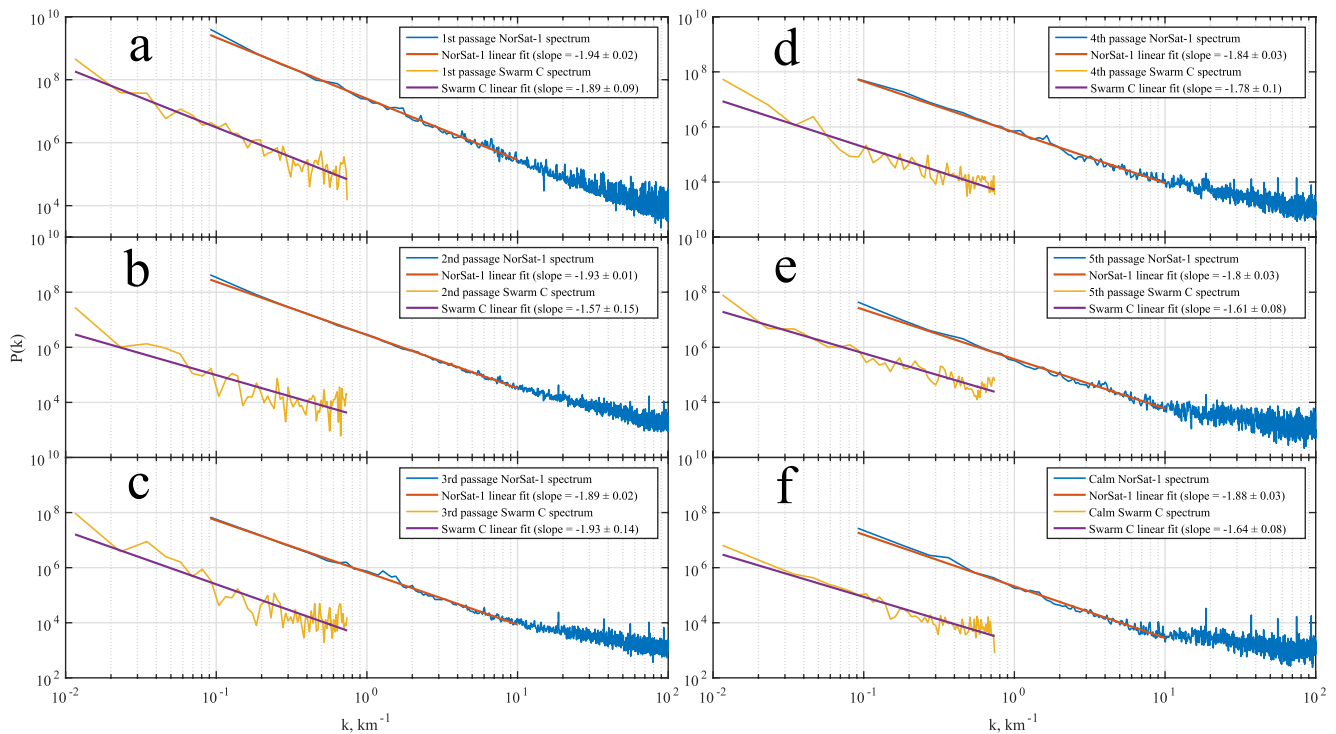


**Figure 3.** The spectra of the electron density inside the polarization jet during the five considered joint passages (at 10, 13, 16, 18, and 21 UT on 20 April 2018) as well as during the passage on a “geomagnetically quiet” day on 19 April 2018, from NorSat-1 (blue line) and Swarm-C (yellow line) as functions of the spatial wavenumber  $k$ . The straight red line marks the linear approximation of the NorSat-1 spectrum up to  $k = 10 \text{ km}^{-1}$ . The purple straight line marks a linear approximation of the Swarm-C spectrum.

$$ROD(t) = \frac{Ne(t + \Delta t) - Ne(t)}{\Delta t} \quad (5)$$

Thus, ROD relates to the temporal variations in density, which can be related to the smallest spatial scales measured by a satellite. Figures 2c and 2d illustrates a comparison of evolutions of the electron density and RODI in 0.1 s for NorSat-1 and in 2 s for Swarm-C. This figure shows that the RODI parameter inside the PJ behaves in a similar way to the electron temperature in Figures 2a and 2b. Four rises in RODI (three strongly pronounced at  $\sim 53.2$ ,  $\sim 52.8$ , and  $\sim 52.5$  which are indicated here by arrows and one weakly pronounced at  $\sim 52.3$  MLAT) coinciding with local dips in electron density correspond to four rises in electron temperature in Figure 2a. An increase in RODI indicates the presence of small-scale electron density irregularities/gradients within strata inside the PJ according to the NorSat-1 data. On the bottom panel, in Figure 2, according to RODI, it is not possible to detect small-scale irregularities in the electron density due to insufficient sampling frequency of the LPs onboard Swarm-C, and an increase in RODI is observed only at the polar wall of the PJ by  $\sim 52.4$  MLAT coinciding with a sharp drop in electron density.

Figures 3a–3e shows the electron density spectra inside the PJ according to data from NorSat-1 and Swarm-C during the five joint flights considered in this work, at 10, 13, 16, 18, and 21 UT on 20 April 2018, and presented as functions of the spatial wave number. For comparison, Figure 3f shows the passage of satellites at 10 UT on 19 April 2018, when the geomagnetic activity was low according to the SME ( $\sim 80 \text{ nT}$ ) and Dst ( $\sim 7 \text{ nT}$ ) indices (hereinafter referred to as “quiet” passage), and without PJ. Since the maximum sampling rate of the instrument on NorSat-1 is 1 kHz, and the Swarm-C density data are at 2 Hz, the NorSat-1 and Swarm-C spectra in Figure 3 lag behind each other on the abscissa and the NorSat-1 spectrum is wider.

Figure 3a shows the electron density spectra according to data from NorSat-1 and Swarm-C inside the PJ during the first considered joint flight of NorSat-1 at 10:11:25–10:11:30 UT and Swarm-C at 10:04:25–10:04:45 UT. As can be seen from Figure 3a, the slope of the NorSat-1 spectrum up to  $k = 10 \text{ km}^{-1}$  during the first passage

is  $-1.94 \pm 0.02$ , while the slope of the Swarm-C spectrum is  $-1.89 \pm 0.09$ . Thus, it can be argued that the slopes of the spectra in the electron density measured with NorSat-1 and Swarm-C are similar within the PJ during the first passage. During the first passage (Figure 3a), at the moment of the highest geomagnetic activity (SME =  $\sim 1,500$  nT), the greatest slope of the spectrum ( $-1.94 \pm 0.02$ ) for NorSat-1 is observed up to  $k = 10 \text{ km}^{-1}$ . Also, during the first passage, the highest values of the spectral power in the NorSat-1 and Swarm-C spectra are observed among the passages considered in this study. At  $k = 0.1 \text{ km}^{-1}$ , the spectral power of the NorSat-1 spectrum is  $5.4 \times 10^{10}$ , at  $k = 10 \text{ km}^{-1}$  is  $2.8 \times 10^5$ . Also, during passages 2, 3, 4, 5, and during the “quiet” passage, a break in the spectrum at  $k = \sim 10 \text{ km}^{-1}$  is noticeable, while Figure 3a shows that during the first passage, there is no break and the spectrum is almost a straight line.

Figure 3b shows the electron density spectra inside the PJ according to the data from NorSat-1 and Swarm-C during the second considered joint passage of NorSat-1 at 13:22:56–13:23:21 UT and Swarm-C at 13:08:15–13:08:45 UT. This figure shows that the slope of the NorSat-1 spectrum up to  $k = 10 \text{ km}^{-1}$  is  $-1.93 \pm 0.01$ . The slope of the Swarm-C spectrum during this passage is the smallest among all the considered passages and is equal to  $-1.57 \pm 0.15$ , which can be explained by the fact that, according to Figure 1a, at the moment when Swarm-C crossed the PJ during the second passage, the geomagnetic activity was the lowest (SME =  $\sim 250$  nT). It is important to note that due to the relatively low resolution of the probe on Swarm, the error in determining the spectrum slope is high. Therefore, the slope of the spectra calculated from the Swarm data has a large scatter of values.

The electron density spectra inside the PJ during the third considered joint passage of NorSat-1 at 16:36:46–16:37:16 UT and Swarm-C at 16:14:30–16:14:50 UT are presented in Figure 3c. The slope of the NorSat-1 spectrum to  $k = 10 \text{ km}^{-1}$  since the previous passages decreased to  $-1.89 \pm 0.02$ , the slope of the Swarm-C spectrum during the third passage was  $-1.93 \pm 0.14$ . In the section  $k > 10 \text{ km}^{-1}$  and  $P \leq 10^2$ , a noticeable break in the NorSat-1 spectrum is observed, which is possibly explained by the presence of high-frequency noise with a power of  $\sim 10^4$ .

Figure 3d shows the electron density spectra inside the PJ during the fourth joint passage of NorSat-1 at 18:13:58–18:14:20 UT and Swarm-C at 17:48:16–17:48:36 UT. The slope of the NorSat-1 spectrum in the section  $k < 10 \text{ km}^{-1}$  has changed since the previous passage and now is  $-1.84 \pm 0.03$ . The slope of the Swarm-C spectrum from the previous passage decreased by 0.15 to  $-1.78 \pm 0.1$ .

Electron density spectra during the fifth considered joint passage of NorSat-1 at 21:27:17–21:27:30 UT and Swarm-C at 20:55:38–20:56:15 UT are shown in Figure 3e. The slope of the NorSat-1 spectrum in the section  $k < 10 \text{ km}^{-1}$  from the previous passage decreased by 0.04 to  $-1.8 \pm 0.03$ . The slope of the Swarm-C spectrum is  $-1.61 \pm 0.08$ . Also, in Figure 3f in the NorSat-1 spectrum, in addition to the break in the section  $k > 10 \text{ km}^{-1}$ , several narrow lines of increased power are visible. Since these lines are visible almost in all spectra at the same frequencies, they are likely caused by high-frequency interference of satellite instruments as well as earlier in Figure 3c.

According to Figures 3 and 1a, with a decrease in the geomagnetic activity and an increase in the passage number, the slope of the NorSat-1 spectrum decreases. At the same time, the slope of the Swarm-C spectrum decreased during the second passage to  $-1.57 \pm 0.15$ , then increased to  $-1.93 \pm 0.14$  during the third passage, and then continued to decrease in subsequent passages. This can be explained by the fact that when Swarm-C crossed the PJ during the second passage, the geomagnetic activity was minimal. Also, according to Figure 3, it can be seen that with an increase in the flight number, the spectral power of the spectra decreases, which, when approaching a value of  $\sim 10^4$ , causes the appearance of a break in the NorSat-1 spectrum at  $k = \sim 10 \text{ km}^{-1}$ .

For comparison with Figures 3a–3e, Figure 3f presents the electron density spectra obtained from NorSat-1 and Swarm during the joint passage of NorSat-1 at 10:26:20–10:26:40 UT and Swarm-C at 10:21:20–10:21:30 UT on a “geomagnetically quiet” day, 19 April 2018. As can be seen in Figure 3f, the slope of the NorSat-1 spectrum during a “quiet” passage is  $-1.88 \pm 0.03$ , which is less than all the considered passages on 20 April 2018, except for the fifth passage, in which the slope of the NorSat-1 spectrum is 0.08 less than the “quiet” flight and amounts to  $-1.8 \pm 0.03$  and for the fourth passage, in which the NorSat-1 spectrum slope is less by 0.04 and equals to  $-1.84 \pm 0.03$ .

#### 4. Discussion and Conclusions

In this paper, the study of the small-scale structure of the PJ in the subauroral region during the geomagnetic activity using the low-orbit satellites, NorSat-1 and Swarm-C, is presented. The results of observations of plasma parameters inside the PJ/SAID were obtained on NorSat-1 using a system of LPs, having a nominal sampling rate of up to 1 kHz, for the first time allowed measurements with such a high temporal resolution. Electron density spectra were obtained from observations at NorSat-1 and Swarm-C and their dynamics were analyzed during the geomagnetic storm on 20 April 2018. A comparative analysis of changes in the electron density and temperature according to the data of NorSat-1 and Swarm-C during their crossing of the PJ demonstrated a similar behavior of the plasma parameters recorded on both satellites. This reaffirms that the NorSat-1 m-NLP and the Swarm-C spherical LP provide adequate results.

As shown by NorSat-1 and Swarm data, PJ is located on relatively low latitudes (52–53 MLAT). According to the Kp index database (Matzka et al., 2021), the average Kp of this storm is 4+, at 6–9 UT is 6 and at 9–12 UT is 6–. In accordance with Karlsson et al. (1998) and He et al. (2012), SAID/PJ at Kp = 6 could reach 50 MLAT. Additionally, according to Foster and Vo (2002), SAPS (which is often located on same latitudes as SAID/PJ) could reach 52–53 MLAT at Kp > 4+. Thus, our study confirms the previously known result that the MLAT of SAID/PJ is changing with the changing of geomagnetic activity.

Note that with the development of geomagnetic activity, an increase in fluctuations in plasma density occurs at all scales. It is demonstrated that small-scale irregularities of the PJ are measured in situ down to hundreds of meters. The intensity of small-scale irregularities also increases with an increase in geomagnetic activity, since during the first passage, at the moment of which the highest geomagnetic activity was observed (SME = ~1,500 nT), the spectrum intensity over the entire range of  $k$  was higher than during other passages.

With a decrease in geomagnetic activity, the slope of the electron density spectrum inside the PJ decreases. In other words, during the development of geomagnetic activity, the role of large-scale effects in the PJ reduces. This is most likely due to the fact that the PJ, which is known to represent narrow fluxes of fast subauroral ion drifts to the west near the projection of the plasmopause at heights of the F-region of the ionosphere, is most noticeably manifested during a geomagnetic substorm/storm against the background of large-scale plasma convection (Galperin, 2002).

In the article by Mishin and Blaunstein (2008), the spectra of plasma irregularities inside SAPS were studied using data from the DMSP F-13 and F-14 satellites, and it was found that the spectra can be well described by a power law with a spectral index in the range:  $-5/3 \geq p_n \geq -2$ . In the present study, we find that the slopes of the spectra for the NorSat-1 data are in the range of  $-1.8 \geq p_n \geq -1.94$ , while for Swarm-C they are in the interval  $-1.51 \geq p_n \geq -1.93$ . It can be seen that the values of the slopes of the spectra in our study are close to the spectral indices given in Mishin and Blaunstein (2008). In Foster and Rich (1998), the spectral power of plasma density as a function of spatial wavenumber from DMSP F-10 observations was presented and the slope was approximately  $-1.5$  for irregularities with scales from 0.6 to 60 km. The authors argued that these spectral characteristics correspond to inhomogeneities associated with the development of the equatorial spread F, and indicated the importance of geomagnetic storms/substorms as a cause of scintillations in mid-latitudes (Foster & Rich, 1998). The mechanism for the generation of this type of plasma irregularities in the subauroral region is still an open question. Since the PJ is accompanied by a strong meridional drift with a velocity exceeding the speed of sound, one should expect the formation of small-scale plasma irregularities in it, caused by various instabilities, for example, Farley-Buneman instability (Farley, 1963). Furthermore, there is a possibility of the development of gradient drift instability (Kadomtsev, 1965), ion frictional heating instability (Keskinen et al., 2004), and ionospheric feedback instability (Watanabe, 2010) in this region, which can also be responsible for the appearance of plasma irregularities (Mishin & Blaunstein, 2008).

It is also worth noting that a strong variability of the electron temperature was found inside the PJ, as well as dips in the electron density, ~0.2 MLAT in size, which coincide with an increase in the electron temperature and in the RODI according to the data from the high-resolution m-NLP on NorSat-1. This may indicate that the PJ consists of several/many strata which include many small-scale irregularities. To test this hypothesis, further detailed studies of the small-scale structure of PJs are required.

## Data Availability Statement

All data used in this study are publicly accessible. Data from Norsat-1 are available on the website (<http://tid.uio.no/plasma/norsat>). Data from the Swarm mission can be accessed through the ESA-website ([https://swarm-diss.eo.esa.int/#swarm/Advanced/Plasma\\_Data/2\\_Hz\\_Langmuir\\_Probe\\_Extended\\_Dataset](https://swarm-diss.eo.esa.int/#swarm/Advanced/Plasma_Data/2_Hz_Langmuir_Probe_Extended_Dataset)). Data from the DMSP mission can be downloaded from NOAA-website (<https://satdat.ngdc.noaa.gov/dmsp/data/f17/>). Geomagnetic activity index data are accessed from the World Geomagnetism Data Center in Kyoto (<http://wdc.kugi.kyoto-u.ac.jp/dstae/index.html>), SuperMAG collaboration (<https://supermag.jhuapl.edu/indices>) and GFZ German Research Centre for Geosciences ([http://www-app3.gfz-potsdam.de/kp\\_index/Kp\\_ap\\_Ap\\_SN\\_F107\\_since\\_1932.txt](http://www-app3.gfz-potsdam.de/kp_index/Kp_ap_Ap_SN_F107_since_1932.txt)). SuperDARN data are obtained from the Virginia Tech SuperDARN website (<http://vt.superdarn.org/tiki-index.php?page=DaViT+Multi+Scan+Plot>).

## Acknowledgments

SuperDARN is a collection of radars funded by national scientific funding agencies of Australia, Canada, China, France, Italy, Japan, Norway, South Africa, the United Kingdom, and the United States. The work is the outcome of the ASTRA - The Arctic Space TRAINing collaboration program, funded by The Norwegian Agency for International Cooperation and Quality Enhancement in Higher Education, Diku (project number CPRU-2017/10068). The work of AAS and AAC was supported by the Theoretical Physics and Mathematics Advancement Foundation "BASIS." The work of AVO was financially supported by the Ministry of Science and Higher Education of Russian Federation. WJM and LBNC received funding from the European Research Council under the European Union's Horizon-2020 research and innovation programme (Grant Agreement No. 866357, POLAR-4DSpace) and the Research Council of Norway (projects No. 275653 and 275655).

## References

- Anderson, P. C., Carpenter, D. L., Tsuruda, K., Mukai, T., & Rich, F. J. (2001). Multisatellite observations of rapid subauroral ion drifts (SAID). *Journal of Geophysical Research*, *106*(A12), 29585–29599. <https://doi.org/10.1029/2001JA000128>
- Anderson, P. C., Hanson, W. B., Heelis, R. A., Craven, J. D., Baker, D. N., & Frank, L. A. (1993). A proposed production model of rapid subauroral ion drifts and their relationship to substorm evolution. *Journal of Geophysical Research*, *98*(A4), 6069–6078. <https://doi.org/10.1029/92JA01975>
- Anderson, P. C., Heelis, R. A., & Hanson, W. B. (1991). The ionospheric signatures of rapid subauroral ion drifts. *Journal of Geophysical Research*, *96*(A4), 5785–5792. <https://doi.org/10.1029/90JA02651>
- Archer, W. E., Gallardo-Lacourt, B., Perry, G. W., St-Maurice, J. P., Buchert, S. C., & Donovan, E. (2019). Steve: The optical signature of intense subauroral ion drifts. *Geophysical Research Letters*, *46*(12), 6279–6286. <https://doi.org/10.1029/2019GL082687>
- Burke, W. J., Maynard, N. C., Hagan, M. P., Wolf, R. A., Wilson, G. R., Gentile, L. C., et al. (1998). Electrodynamics of the inner magnetosphere observed in the dusk sector by CRRES and DMSP during the magnetic storm of June 4–6, 1991. *Journal of Geophysical Research*, *103*(A12), 29399–29418. <https://doi.org/10.1029/98JA02197>
- Burke, W. J., Rubin, A. G., Maynard, N. C., Gentile, L. C., Sultan, P. J., Rich, F. J., et al. (2000). Ionospheric disturbances observed by DMSP at middle to low latitudes during the magnetic storm of June 4–6, 1991. *Journal of Geophysical Research*, *105*(A8), 18391–18405. <https://doi.org/10.1029/1999JA000188>
- Chernyshov, A. A., Chuginin, D. V., Frolov, V. L., Clausen, L. B. N., Miloch, W. J., & Mogilevsky, M. M. (2020). In situ observations of ionospheric heating effects: First results from a joint SURA and NorSat-1 experiment. *Geophysical Research Letters*, *47*(13), e2020GL088462. <https://doi.org/10.1029/2020GL088462>
- de Keyser, J. (2000). Storm-time energetic particle penetration into the inner magnetosphere as the electromotive force in the subauroral ion drift current circuit. *Washington DC American Geophysical Union Geophysical Monograph Series*, *118*, 261–265. <https://doi.org/10.1029/GM118p0261>
- Farley, D. T. (1963). Two-stream plasma instability as a source of irregularities in the ionosphere. *Physical Review Letters*, *10*(7), 279–282. <https://doi.org/10.1103/PhysRevLett.10.279>
- Figueiredo, S., Karlsson, T., & Marklund, G. (2004). Investigation of subauroral ion drifts and related field-aligned currents and ionospheric Pedersen conductivity distribution. *Annales Geophysicae*, *22*(3), 923–934. <https://doi.org/10.5194/angeo-22-923-2004>
- Foster, J. C., & Burke, W. J. (2002). SAPS: A new categorization for sub-auroral electric fields. *EOS Transactions*, *83*(36), 393. <https://doi.org/10.1029/2002EO000289>
- Foster, J. C., Erickson, P. J., Coster, A. J., Goldstein, J., & Rich, F. J. (2002). Ionospheric signatures of plasmaspheric tails. *Geophysical Research Letters*, *29*(13), 1623. <https://doi.org/10.1029/2002GL015067>
- Foster, J. C., & Rich, F. J. (1998). Prompt midlatitude electric field effects during severe geomagnetic storms. *Journal of Geophysical Research*, *103*(A11), 26367–26372. <https://doi.org/10.1029/97JA03057>
- Foster, J. C., & Vo, H. B. (2002). Average characteristics and activity dependence of the SubAuroral Polarization Stream. *Journal of Geophysical Research*, *107*(A12), 1475. <https://doi.org/10.1029/2002JA009409>
- Gallardo-Lacourt, B., Nishimura, Y., Lyons, L. R., Mishin, E. V., Ruohoniemi, J. M., Donovan, E. F., et al. (2017). Influence of auroral streamers on rapid evolution of ionospheric saps flows. *Journal of Geophysical Research: Space Physics*, *122*(12), 12406–12420. <https://doi.org/10.1002/2017JA024198>
- Galperin, Y. I. (2002). Polarization jet: Characteristics and a model. *Annales Geophysicae*, *20*(3), 391–404. <https://doi.org/10.5194/angeo-20-391-2002>
- Gal'perin, Y. I., Ponomarev, V. N., & Zosimova, A. G. (1973). Direct measurements of drift rate of ions in upper atmosphere during a magnetic storm. I. Problems of method and some results of measurements during magnetically quiet period. *Cosmic Research*, *11*(2), 240.
- Gal'perin, Y. I., Ponomarev, V. N., & Zosimova, A. G. (1974). Plasma convection in the polar ionosphere. *Annales Geophysicae*, *30*(1), 1–7.
- Goldstein, J., Sandel, B. R., Hairston, M. R., & Reiff, P. H. (2003). Control of plasmaspheric dynamics by both convection and sub-auroral polarization stream. *Geophysical Research Letters*, *30*(24), 2243. <https://doi.org/10.1029/2003GL018390>
- He, F., Zhang, X.-X., Chen, B., & Fok, M. (2012). Plasmaspheric trough evolution under different conditions of subauroral ion drift. *Science in China E: Technological Sciences*, *55*(5), 1287–1294. <https://doi.org/10.1007/s11431-012-4781-1>
- He, F., Zhang, X.-X., Wang, W., & Chen, B. (2016). Double-peak subauroral ion drifts (DSAIDs). *Geophysical Research Letters*, *43*(11), 5554–5562. <https://doi.org/10.1002/2016GL069133>
- Hoang, H., Clausen, L. B. N., Røed, K., Bekkeng, T. A., Trondsen, E., Lybekk, B., et al. (2018). The multi-needle Langmuir probe system on board NorSat-1. *Space Science Reviews*, *214*(4), 75. <https://doi.org/10.1007/s11214-018-0509-2>
- Jacobsen, K. S., Pedersen, A., Moen, J. I., & Bekkeng, T. A. (2010). A new Langmuir probe concept for rapid sampling of space plasma electron density. *Measurement Science and Technology*, *21*(8), 085902. <https://doi.org/10.1088/0957-0233/21/8/085902>
- Jin, Y., Spicher, A., Xiong, C., Clausen, L. B. N., Kervalishvili, G., Stolle, C., & Miloch, W. J. (2019). Ionospheric plasma irregularities characterized by the swarm satellites: Statistics at high latitudes. *Journal of Geophysical Research: Space Physics*, *124*(2), 1262–1282. <https://doi.org/10.1029/2018JA026063>

- Kadomtsev, B. B. (1965). *Plasma turbulence*. Academic Press.
- Karlsson, T., Marklund, G. T., Blomberg, L. G., & Mälkki, A. (1998). Subauroral electric fields observed by the Freja satellite: A statistical study. *Journal of Geophysical Research*, *103*(A3), 4327–4341. <https://doi.org/10.1029/97JA00333>
- Keskinen, M. J., Basu, S., & Basu, S. (2004). Midlatitude sub-auroral ionospheric small scale structure during a magnetic storm. *Geophysical Research Letters*, *31*(9), L09811. <https://doi.org/10.1029/2003GL019368>
- Khalipov, V. L., Galperin, Y. I., Stepanov, A. E., & Bondar, E. D. (2003). Formation of polarization jet during injection of ions into the inner magnetosphere. *Advances in Space Research*, *31*(5), 1303–1308. [https://doi.org/10.1016/S0273-1177\(03\)00016-4](https://doi.org/10.1016/S0273-1177(03)00016-4)
- Khalipov, V. L., Stepanov, A. E., Kotova, G. A., & Bondar, E. D. (2016). Formation of polarization jet during injection of ions into the inner magnetosphere. *Geomagnetism and Aeronomy*, *56*(2), 187–193. <https://doi.org/10.1134/S0016793216020080>
- Knudsen, D. J., Burchill, J. K., Buchert, S. C., Eriksson, A. I., Gill, R., Wahlund, J. E., et al. (2017). Thermal ion imagers and Langmuir probes in the Swarm electric field instruments. *Journal of Geophysical Research*, *122*(2), 2655–2673. <https://doi.org/10.1002/2016JA022571>
- Koustov, A. V., Drayton, R. A., Makarevich, R. A., McWilliams, K. A., St-Maurice, J.-P., Kikuchi, T., & Frey, H. U. (2006). Observations of high-velocity SAPS-like flows with the King Salmon SuperDARN radar. *Annales Geophysicae*, *24*(6), 1591–1608. <https://doi.org/10.5194/angeo-24-1591-2006>
- Makarevich, R. A., Kellerman, A. C., Devlin, J. C., Ye, H., Lyons, L. R., & Nishimura, Y. (2011). Saps intensification during substorm recovery: A multi-instrument case study. *Journal of Geophysical Research*, *116*(A11). <https://doi.org/10.1029/2011JA016916>
- Matzka, J., Bronkalla, O., Tornow, K., Elger, K., & Stolle, C. (2021). *Geomagnetic kp index*. v. 1.0. GFZ Data Services. <https://doi.org/10.5880/Kp.0001>
- Maynard, N. C. (1978). On large poleward-directed electric fields at sub-auroral latitudes. *Geophysical Research Letters*, *5*(7), 617–618. <https://doi.org/10.1029/GL005i007p00617>
- Mishin, E. V. (2013). Interaction of substorm injections with the subauroral geospace: 1. Multispacecraft observations of SAID. *Journal of Geophysical Research*, *118*(9), 5782–5796. <https://doi.org/10.1002/jgra.50548>
- Mishin, E. V., & Blaunstein, N. (2008). Irregularities within subauroral polarization stream-related troughs and GPS radio interference at midlatitudes. *Washington DC American Geophysical Union Geophysical Monograph Series*, *181*, 291–295. <https://doi.org/10.1029/181GM26>
- Mishin, E. V., Burke, W. J., Huang, C. Y., & Rich, F. J. (2003). Electromagnetic wave structures within subauroral polarization streams. *Journal of Geophysical Research*, *108*(A8), 1309. <https://doi.org/10.1029/2002JA009793>
- Mishin, E. V., Nishimura, Y., & Foster, J. (2017). SAPS/SAID revisited: A causal relation to the substorm current wedge. *Journal of Geophysical Research*, *122*(8), 8516–8535. <https://doi.org/10.1002/2017JA024263>
- Nishitani, N., Ruohoniemi, J. M., Lester, M., Baker, J. B. H., Koustov, A. V., Shepherd, S. G., et al. (2019). Review of the accomplishments of mid-latitude super dual auroral radar network (SuperDARN) HF radars. *Progress in Earth and Planetary Science*, *6*(27). <https://doi.org/10.1186/s40645-019-0270-5>
- Rowland, D. E., & Wygant, J. R. (1998). Dependence of the large-scale, inner magnetospheric electric field on geomagnetic activity. *Journal of Geophysical Research*, *103*(A7), 14959–14964. <https://doi.org/10.1029/97JA03524>
- Sinevich, A. A., Chernyshov, A. A., Chugunin, D. V., Miloch, W. J., & Mogilevsky, M. M. (2021). Studying the small-scale structure of a polarization jet during the April 20, 2018 geomagnetic storm. *Solar-Terrestrial Physics*, *7*, 17–26. <https://doi.org/10.12737/stp-71202103>
- Smiddy, M., Kelley, M. C., Burke, W., Rich, F., Sagalyn, R., Shuman, B., et al. (1977). Intense poleward-directed electric fields near the ionospheric projection of the plasmapause. *Geophysical Research Letters*, *4*(11), 543–546. <https://doi.org/10.1029/GL004i011p00543>
- Spiro, R. W., Heelis, R. A., & Hanson, W. B. (1979). Rapid subauroral ion drifts observed by Atmosphere Explorer C. *Geophysical Research Letters*, *6*(8), 657–660. <https://doi.org/10.1029/GL006i008p00657>
- Stepanov, A. E., Khalipov, V. L., Golikov, I. A., & Bondar, E. D. (2017). *Polarized jet: Narrow and fast drifts of subauroral ionospheric plasma*. Nauka Publ.
- Stepanov, A. E., Khalipov, V. L., Kobayakova, S. E., & Kotova, G. A. (2019). Results of observations of ionospheric plasma drift in the polarization jet region. *Geomagnetism and Aeronomy*, *59*, 539–542. <https://doi.org/10.1134/S001679321905013X>
- Watanabe, T.-H. (2010). Feedback instability in the magnetosphere-ionosphere coupling system: Revisited. *Physics of Plasmas*, *17*(2), 022904. <https://doi.org/10.1063/1.3304237>
- Wei, D., Yu, Y., Ridley, A. J., Cao, J., & Dunlop, M. W. (2019). Multi-point observations and modeling of subauroral polarization streams (SAPS) and double-peak subauroral ion drifts (DSAIDs): A case study. *Advances in Space Research*, *63*(11), 3522–3535. <https://doi.org/10.1016/j.asr.2019.02.004>
- Yeh, H. C., Foster, J. C., Rich, F. J., & Swider, W. (1991). Storm time electric field penetration observed at mid-latitude. *Journal of Geophysical Research*, *96*(A4), 5707–5721. <https://doi.org/10.1029/90JA02751>